frontiers | Frontiers in Marine Science

TYPE Original Research
PUBLISHED 13 December 2022
DOI 10.3389/fmars.2022.1092451

OPEN ACCESS

EDITED BY
Peng Jin,
University of Guangzhou, China

REVIEWED BY
Kai Xu,
Jimei University, China
Hongzhi He,
South China Agricultural University, China

*CORRESPONDENCE
Wenzhou Xiang
xwz@scsio.ac.cn

SPECIALTY SECTION
This article was submitted to Global Change and the Future Ocean, a section of the journal Frontiers in Marine Science

RECEIVED 08 November 2022
ACCEPTED 28 November 2022
PUBLISHED 13 December 2022

CITATION
Wang N, Lv J, Yang F, Li T, Wu H, Li C, Pei H, Wu H and Xiang W (2022) Effects of seawater acidification and solar ultraviolet radiation on photosynthetic performances and biochemical compositions of *Rhodosorus* sp. SCSIO-45730. *Front. Mar. Sci.* 9:1092451. doi: 10.3389/fmars.2022.1092451

Effects of seawater acidification and solar ultraviolet radiation on photosynthetic performances and biochemical compositions of *Rhodosorus* sp. SCSIO-45730

Na Wang[1,2], Jinting Lv[1,2], Fangfang Yang[1,3], Tao Li[1,3], Hualian Wu[1,3], Chulin Li[1,2], Haiwei Pei[1,2], Houbo Wu[1,3] and Wenzhou Xiang[1,3]*

[1]Key Laboratory of Tropical Marine Bio-resources and Ecology, RNAM Center for Marine Microbiology, South China Sea Institute of Oceanology, Chinese Academy of Sciences, Guangzhou, China, [2]University of Chinese Academy of Sciences, Beijing, China, [3]Southern Marine Science and Engineering Guangdong Laboratory, Guangzhou, China, [4]Guangdong Key Laboratory of Marine Materia Medica, RNAM Center for Marine Microbiology, South China Sea Institute of Oceanology, Chinese Academy of Sciences, Guangzhou, China

Ocean acidification (OA) caused by rising atmospheric CO_2 concentration and solar ultraviolet radiation (UVR) resulting from ozone depletion may affect marine organisms, but little is known regarding how unicellular *Rhodosorus* sp. SCSIO-45730, an excellent species resource containing various biological-active compounds, responds to OA and UVR. Therefore, we conducted a factorial coupling experiment to unravel the combined effects of OA and UVR on the growth, photosynthetic performances, biochemical compositions and enzyme activities of *Rhodosorus* sp. SCSIO-45730, which were exposed to two levels of CO_2 (LC, 400 µatm, current CO_2 level; HC, 1000 µatm, future CO_2 level) and three levels of UVR (photosynthetically active radiation (PAR), PAR plus UVA, PAR plus UVB) treatments in all combinations, respectively. Compared to LC treatment, HC stimulated the relative growth rate (RGR) due to higher optimum and effective quantum yields, photosynthetic efficiency, maximum electron transport rates and photosynthetic pigments contents regardless of UVR. However, the presence of UVA had no significant effect but UVB markedly reduced the RGR. Additionally, higher carbohydrate content and lower protein and lipid contents were observed when *Rhodosorus* sp. SCSIO-45730 was cultured under HC due to the ample HCO_3^- applications and active stimulation of metabolic enzymes of carbonic anhydrase and nitrate reductase, thus resulting in higher TC/TN. OA also triggered the production of reactive oxygen species (ROS), and the increase of ROS coincided approximately with superoxide dismutase and catalase activities, as well as phenols contents. However, UVR induced photochemical inhibition and

damaged macromolecules, making algal cells need more energy for self-protection. Generally, these results revealed that OA counteracted UVR-related inhibition on *Rhodosorus* sp. SCSIO-45730, adding our understanding of the red algae responding to future global climate changes.

KEYWORDS

***rhodosorus*, seawater acidification, ultraviolet radiation, photosynthetic performance, biochemical composition, enzyme activity**

1 Introduction

Owing to fossil fuel combustion emissions and human activities after the industrial revolution, the atmospheric CO_2 concentration has raised sharply to 400 μatm at the current stage (Gao et al., 2020). According to this trend, the level of CO_2 is predicted to amount to 1000 μatm by the end of 2100 (Wei et al., 2021). On the other hand, the ocean can take in about 1/3 of the atmospheric CO_2, which leads to a change in seawater carbonate chemistry, resulting in ocean acidification (OA) (Zhang et al., 2022). It is well known that OA is reflected in the increase of dissolved free CO_2, HCO_3^- and H+, and the decrease in pH and CO_3^{2-}. Studies have highlighted that OA can complexly influence the growth, photosynthetic performances, biochemical compositions, nutrient assimilation and enzyme activity of various algal groups or species (Li et al., 2017). OA had positive impacts on the growth and photosynthesis of different kinds of marine algae, such as *Gracilariopsis lemaneiformis* (Liu et al., 2020), *Chlorella sorokiniana* (Sun et al., 2016) and *Chaetoceros muelleri* (Liang et al., 2020). However, literature also had shown that an increased CO_2 concentration significantly suppressed the growth and photosynthetic rate of *Ulva linza* (Gao et al., 2018) and *Alexandrium tamarense* (Guan et al., 2018), while there was no obvious effect on *Sargassum fusiforme* (Jiang et al., 2019). Therefore, it can be concluded that the impacts of OA on marine algae might be positive, neutral, or negative, which may be because each species possesses different inorganic carbon utilization tactics (Li et al., 2017).

An increase in exposure to photosynthetically active radiation (PAR, 400–700 nm) and solar ultraviolet radiation (UVR, 280-400 nm) due to ozone depletion and the increase of shoaling in the upper mixed layer of the ocean is another global environmental threat to marine algae. It has been suggested that UVR can bring extensively deleterious influences on the growth, physiological performances and primary production of algae (Li et al., 2022a). For instance, excessive UVB (280-315 nm) impairs DNA and PSII protein synthesis of phytoplankton, inhibits its growth and photosynthetic activity, and stimulates the increase of reactive oxygen species (ROS) and photoprotective pigments (Yu et al., 2022). Furthermore, membrane proteins can also be damaged by UVB, limiting nutrient uptake and carbon assimilation (Chen et al., 2015). However, moderate UVA (315-400 nm) has positive effects on marine algae, for example, enhancement of photosynthetic rates, photosynthetic carbon fixation and UVB-induced photo-repair process (Jiang et al., 2022). The study also has shown that differences in the sensitivity of marine algae on UVR depend on species (Davison et al., 2007), so more work needs to be done to reveal the response of phytoplankton to a rise in UVR. Additionally, reports have studied the effects of single-factor OA or UVR irradiation on the growth, physiological and ecological functions of marine algae, but combined effects have yet to be fully understood and the reported results are still in debate (Gao et al., 2020; Ji and Gao, 2021). Gao and Zheng (2010) reported that elevated CO_2 and UVR synergistically inhibited the chlorophyll a and phycobiliproteins of *Corallina sessilis*. The increase in CO_2 concentration had little effect on the growth rate of *Cylindrotheca closterium f. minutissima* and there was no significant correlation with UVR (Wu et al., 2012).

Marine microalgae possess a large number of polysaccharides, proteins, essential fatty acids, vitamins, mineral oxides and other nutrients with nontoxicity, uniqueness, biodegradability, biocompatibility and high value, thus attracting the attention of researchers worldwide (Raposo et al., 2013; Zhang et al., 2019; Li et al., 2022b). Among them, a carbohydrate-rich microalgal strain, *Rhodosorus* sp. SCSIO-45730 belonging to unicellular red algae in the division Rhodophyta or red algae has received attention as a promising feedstock of biochemistry, biomass energy resources and pharmacology (Wang et al., 2022b). Dai et al. (2020) reported the productivities of total carbohydrates and β-glucans of *Rhodosorus* sp. SCSIO-45730 reached 242.6 mg L^{-1} day^{-1} and 108.1 mg L^{-1} day^{-1}, respectively, which were the highest among reported microalgal strains. Simultaneously, the existing research showed that the purified *Rhodosorus* sp. SCSIO-45730 polysaccharides (RSP) fractions were called RSP-1, PSR-2 and RSP-3, respectively. Among them, RSP-1 and RSP-3 exhibited marked antioxidant activities, and RSP-2 demonstrated strong hypoglycemia activity (Wang et al., 2022a). In addition, the

biomass of *Rhodosorus* sp. SCSIO-45730 reached 12.3 g L^{-1} in the photobioreactor, which was much higher than those for many microalgae cultured in the same reactors (Dai et al., 2020; Sero et al., 2020). Meanwhile, *Rhodosorus* sp. SCSIO-45730 showed ultralow harvest cost by chitosan bio-flocculant, contributing to the commercial production of this algal (Dai et al., 2020). However, it is not known how *Rhodosorus* sp. SCSIO-45730 copes with predicted climate change conditions, such as the interaction between OA and enhanced UVR.

Therefore, we systematically conducted a factorial coupling batch culture experiment to unravel the interactive effects of OA and UVR on the growth, photosynthetic performances, biochemical compositions and enzyme activities of *Rhodosorus* sp. SCSIO-45730. Algal cells were incubated in 16-day trials under six treatments, which included two levels of CO_2 (LC, 400 µatm, current CO_2 level; HC, 1000 µatm, future CO_2 level) and three levels of UVR (photosynthetically active radiation (PAR), PAR plus UVA, PAR plus UVB) treatments in all combinations, respectively. Meanwhile, we also assessed whether there was synergy or antagonism between OA and UVB on the strain.

2 Materials and methods

2.1 Algal collection and culture

Rhodosorus sp. SCSIO-45730 was isolated from Xisha Islands, South China Sea (111°45.000′ E, 16°28.471′ N) by our laboratory (Wang et al., 2022b). The preliminary culture was carried out by incubating the strain in 1500-mL vertical glass bubble column photobioreactors (6.0 cm × 60 cm) containing seawater medium composed of 17.6 mM $NaNO_3$, 0.69 mM $K_2HPO_4{\cdot}3H_2O$, 0.48 mM $NaHCO_3$, 11.7 µM $FeCl_3{\cdot}6H_2O$, 11.7 µM $Na_2EDTA{\cdot}2H_2O$, 0.91 µM $MnCl_2{\cdot}4H_2O$, 0.08 µM $ZnSO_4{\cdot}7H_2O$, 0.04 µM $CoCl_2{\cdot}6H_2O$, 0.04 µM $CuSO_4{\cdot}5H_2O$ and 0.02 µM $Na_2MoO_4{\cdot}2H_2O$ in 28‰ seawater at 25°C and a continuous illumination (Wang et al., 2022b). The culture medium was aerated with ambient air (400 µatm, LC) and elevated CO_2 (1000 µatm, HC) at 1 L min^{-1} continuously for pre-acclimation incubation for 8 days. The concentration of CO_2 at 1000 µatm was attained by mixing pure CO_2 with air.

2.2 Experimental setup and treatments

To explore the combined effects of OA and UVR on *Rhodosorus* sp. SCSIO-45730, we used the pre-acclimation incubation algal strains to implement a 2×3 factorial coupling test for 16-day batch culture. There were 18 vertical glass bubble column photobioreactors (algae in the log phase with an initial OD_{750} of 0.3 in 1.2 L seawater per photobioreactor) divided into six treatment groups with three independent biological replicates (Table 1). The first factor was pCO_2 level: LC and HC, which represented current atmospheric pCO_2 and the estimated values at 2100, respectively. The second factor was UVR treatment. For the control treatment (PAR), fluorescent lamps at 180 µmol photons m^{-2} s^{-1} provided the light and no further UV lamp was used. Concerning UVA treatment (PAR+UVA), the UV-A lamp used in the experiment has a power of 8 W, a spectral emission range of 280-400 nm and a peak value of 365 nm. The outer surface of the UV-A lamp was covered with a quartz glass tube and the ultraviolet transmittance is 95%, forming an integrated submersible lamp (Beijing Zhongyi Boten Technology Co., Ltd., China). For UVB treatment (PAR+UVB), the UV-B lamp with a power of 8 W, a spectral emission range of 280-320 nm, and a peak of 308 nm was wrapped with a cellulose acetate film to remove short-wave radiation below 290 nm. The UV-B lamp tube also had a quartz glass tube with a UV transmittance of 95% to form an integrated diving lamp (Beijing Zhongyi Boteng Technology Co., Ltd., China). UV dose was measured using an LS125 multi-probe UV radiation meter (Shenzhen Linshang Technology Co., Ltd., China). During the experiment, UVA and UVB diving lamps were separately inserted into the medium (Supplementary Figure S1), and the irradiation time was set to 90 min and 80 min, and the corresponding total radiation doses were 149.91 kJ m^{-2} and 7.47 kJ m^{-2}, respectively. From the first day, the algae medium was treated with UV radiation every 48 h until the end of the 16-day culture cycle.

The parameters of carbonate systems in seawater were monitored at the beginning of the batch culture. The temperature and salinity were detected by TES-1332A digital luminance meter and handheld salinity refractometer, respectively. A portable pH meter was used to measure the pH after calibrated by three standard buffer solutions (pH 4.02, 7.00 and 9.21). The total alkalinity (TA) was measured by acid

TABLE 1 2×3 factorial coupling experiments of CO_2 concentration and UV radiation.

Treatments (pCO_2 ×UV radiation)	Seawater pCO_2 (ppm)	UV radiation
LC+PAR	400	PAR alone
LC+PAR+UVA	400	PAR+UVA
LC+PAR +UVB	400	PAR+UVB
HC+PAR	1000	PAR alone
HC+PAR +UVA	1000	PAR+UVA
HC+PAR +UVB	1000	PAR+UVB

standard solution titration with methyl orange as an indicator based on Chinese Standard GB/T8538-1995. According to the known values of temperature, salinity, pH, TA and pCO_2 in culture mediums, HCO^{3-}, CO_3^{2-} and CO_2 were attained by CO_2SYS software (Pierrot et al., 2006).

2.3 Growth measurement

The growth of the strain was measured by biomass dry weight (DW) at the beginning and the end of the test. A 5-mL culture sample was filtered through a pre-weighed 0.45-μm membrane filter, washed three times with deionized water, and dried at 80 °C overnight to reweighed. Furthermore, we calculated the relative growth rate (RGR, % d^{-1}) based on the following formula:

$$RGR = [(\ln B_{16} - \ln B_0)/16] \times 100 \quad (1)$$

wherein B_{16} and B_0 are the DW on day 16 and day 0, respectively.

2.4 Chlorophyll fluorescence measurement

FMS-2 Pulse Modulation Fluorometer (Hansha scientific instruments, China) was used to determine the photosynthetic performances of *Rhodosorus* sp. SCSIO-45730 on day 16. A red light was considered as the modulated light. The Fv/Fm was measured at saturation pulse after 30 min of dark adaption. The rapid light curve (RLC) was determined under 7 levels of actinic light (0, 200, 400, 580, 870, 980 and 1220 μmol photons m^{-2} s^{-1}). The relative electron transport rates (rETR), maximum electron transport rate ($rETR_{max}$), apparent photosynthetic efficiency (α) and saturation light intensity (I_k) are important chlorophyll fluorescence parameters that were calculated by the following equation:

$$rETR = \Phi PSII \times 0.84 \times 0.5 \times A \quad (2)$$

where ΦPSII is the effective photosynthetic quantum yield; the values of 0.84 and 0.5 represent the ambient light quanta absorbed by the sample and the ratio of absorbed light energy to the total incident light energy, respectively; A stands for the light intensity (μmol photons m^{-2} s^{-1}). RLC was obtained by the fitting formula (Eilers and Peeters, 1988):

$$rETR = I/(aI^2 + bI + c) \quad (3)$$

where I is the actinic light level (μmol photons m-2 s-1) and a, b and c were constants.

$$rETR_{max} = 1/(b + 2\sqrt{a \times c}) \quad (4)$$

$$\alpha = 1/c \quad (5)$$

$$I_k = c/(b + 2\sqrt{a \times c}) \quad (6)$$

2.5 Microalgal biochemical compositions determination

The algae cultures at day 16 were collected by centrifugation at 8 000 r min^{-1} for 5 min and washed with deionized water three times. After freeze-drying (FD-1-50, Beijing Boyikang Laboratory Instrument Co., Ltd., China), the algal powder was obtained and kept at -20 °C for further biochemical experiments.

2.5.1 Pigment contents

A 10-mg algal tissue was extracted by pure acetone (5 mL) at 4 °C for 48 h in darkness. The mixtures were then centrifuged at 5000 r min^{-1} for 5min. The absorbances of supernatant were obtained at 662, 645 and 470 nm by TU-1810 spectrophotometry (Persee Instrument Co., Ltd., China). The contents of chlorophyll a (Chl a) and total carotenoids (Car) were calculated according to the equations reported by Li et al. (2020b).

2.5.2 Phycobiliprotein contents

A 20-mg freeze-dried biomass was extracted with a 0.1 M phosphate buffer (pH 6.70), sonicated for 10 min, and then freeze-thawed repeatedly until no obvious red color appeared. The absorbances of the supernatant at 565, 620 and 650 nm were measured using a TU-1810 spectrophotometer (Persee Instrument Co., Ltd., China). The concentrations of R-phycocyanin (R-PC), phycocyanin (PC) and phycoerythrin (PE) were estimated by the method proposed by Tandeau de Marsac and Houmard (1988).

2.5.3 Total carbohydrate content

A 10-mg lyophilized algae powder was extracted by 0.5 N H_2SO_4 at 80 °C for 2 h, and repeated three times. The phenol-sulfuric acid method was employed to determine total carbohydrate content (Dubois et al., 1956).

2.5.4 Crude protein content

A 50-mg lyophilized cell sample was extracted with 0.5 N NaOH at 80 °C for 2 h and repeated three times. The Lowry method was used to measure the amount of crude protein (Lowry, 1951), and Nanjing Jiancheng Biological Engineering Institute provided the protein quantitation kit.

2.5.5 Total lipids content

An 80-mg freeze-dried biomass was extracted by dimethyl sulfoxide-methanol (1:9, *v/v*) and hexane-diethyl ether (1:1, *v/v*)

based on Khozin-Goldberg method with some modification (Khozin-Goldberg et al., 2005). The gravimetric methods determined the total lipids content and normalized on the DW of samples.

2.5.6 Phenols content

A 200-mg algal material was extracted with 2.5 mL of 80% methanol. The extracts were rotated continuously at 4 °C overnight and centrifuged at 8000 r min^{-1} for 15 min. The supernatants were collected to determine the phenolic content by the Folin-Ciocalteu reagent method (Foo et al., 2017). Phenolic quantification was measured and expressed as mg per g of dry biomass based on a standard curve of gallic acid.

2.6 Determination of total carbon, total nitrogen and C/N ratio

A 50-mg sample was used for total carbon and nitrogen analysis by Elemental Vario PYRO CUBE (Elemental company, Germany) equipped with a 120-position autosampler. The samples were decomposed by catalytic oxidation in a pure oxygen atmosphere at 850 °C. The non-detecting gas in the generated gas was removed, and the detected gas components were detected by a thermal conductivity detector after being separated by a special adsorption column. Helium was used as a carrier and purge gas. Acetanilide was considered as the standard sample and the results were indicated as a percentage relative to the DW of the sample.

2.7 Enzymatic activities

A 40-mL algal sample was collected by centrifugation on day 16 and rapidly resuspended in 80 ml of 0.1 M phosphate buffer (pH 7.5). An ultrasonic disruptor (Sonicator S-4000, Misonix Company, USA) was employed to broke cells at 4 °C. The crushing procedure was under 3 pulses with 5-s intervals at a power of 20 W for 5 min. Superoxide dismutase (SOD), catalase (CAT), carbonic anhydrase (CA) and nitrate reductase (NR) activities were investigated by ELISA Kits (Hengyuan biological, Shanghai, China), and the operations followed the manufacturer's instructions.

2.8 Statistical analyses

Data are presented as mean and standard deviations of triplicate experiments (n = 3) using a statistical system (origin 8.5). One-way analysis of variance (ANOVA) was adopted to decide the differences of treatments under the same pCO_2 levels but at different UVR conditions, and two-way ANOVA was performed to analyze interactive effects between pCO_2 levels and UVR on carbonate system parameters, RGR, photosynthesis performances, biochemical compositions and related enzyme activities. The statistical program IBM SPSS statistics 25 was adopted to analyze data. Tukey's honestly significant difference (HSD) analysis was employed to conduct *post hoc* comparisons and $p < 0.05$ showed a significant difference.

3 Results

3.1 Carbonate system

The carbonate system parameters of each treatment were measured at the beginning of the batch culture period (Table 2). OA had a significant impact on pH, TA, CO_2, HCO_3^- and CO_3^{2-} of seawater ($p<0.01$), while UVR or interaction between OA and UVR ($p>0.05$) had no significant effect (Supplementary Table S1). The average pH levels dropped from 8.25 to 7.86 with the pCO_2 level increasing from 400 to 1000 µatm. In comparison with the LC treatment, the average TA and CO_3^{2-} concentration decreased from 2444.58- 2447.51 µmol kg^{-1} to 2361.18-2363.13 µmol kg^{-1} and from 267.86-275.27 µmol kg^{-1} to 119.97-122.72 µmol kg^{-1}, respectively. Nevertheless, the concentrations of CO_2 and HCO_3^- under HC conditions were ~16.55 and ~2068.06 µmol kg^{-1}, which were 66.47% and 12.82%, respectively, higher than LC treatments.

TABLE 2 Seawater carbonate system parameters under ambient CO_2 (LC: 400 uatm) and elevated CO_2 (HC: 1000 ppm), treated with different radiation treatments (PAR; PAR+UVA; PAR+UVB).

Treatments	pCO_2 (µatm)	pH	TA (µmol kg^{-1})	CO_2 (µmol kg^{-1})	HCO_3^- (µmol kg^{-1})	CO_3^{2-} (µmol kg^{-1})
LC+PAR	400±0.00	8.25±0.01	2444.58±7.34	5.71±0.10	1802.93±2.25	270.16±4.21
LC+PAR+UVA	399±1.41	8.26±0.01	2447.51±3.18	5.55±0.12	1793.98±10.40	275.27±3.02
LC+PAR+UVB	401±0.71	8.24±0.00	2445.25±6.38	5.80±0.02	1809.02±4.90	267.86±0.73
HC+PAR	1000±0.00	7.86±0.01	2363.13±4.25	16.55±0.68	2068.06±12.73	122.72±3.51
HC+PAR+UVA	999.5±0.81	7.85±0.00	2361.18±7.06	17.00±0.05	2072.63±6.32	119.97±0.37
HC+PAR+UVB	999±1.40	7.86±0.01	2362.27±5.81	16.55±0.69	2067.29±14.13	122.67±3.43

TA indicates total alkalinity. Data are mean ± standard deviation (n = 3).

3.2 Growth characteristics

Two-way ANOVA showed that OA or UVR alone had significant effects on RGR in *Rhodosorus* sp. SCSIO-45730, while their interactions had no significant effect (Supplementary Table S2). Figure 1 showed that the elevated CO_2 enhanced the RGR of *Rhodosorus* sp. SCSIO-45730 by 50.79%, 31.89% and 35.41%, respectively, under PAR, PAR +UVA and PAR+UVB. Compared with PAR and PAR+UVA treatments, PAR+UVB represented inhibition effects on the RGR of *Rhodosorus* sp. SCSIO-45730 regardless of CO_2 treatments. In particular, the RGR was the lowest with values of 11.84% day^{-1} under LC+PAR+UVB treatment.

3.3 Chlorophyll fluorescence parameters

We observed the effects of CO_2 concentrations and UVR on the RLC in *Rhodosorus* sp. SCSIO-45730 as shown in Figure 2. The photosynthetic parameters of *Rhodosorus* sp. SCSIO-45730 estimated by RLC were shown in Figure 3. OA and UVR had significant interactive effects on Fv/Fm, rETRm and I_k, and no interactive effect existed on α (Supplementary Table S3). Under HC treatment, the Fv/Fm significantly increased from 0.06-0.24 (LC) to 0.29-0.43, and α from 0.01-0.02 (LC) to 0.05-0.07, and rETRm was from 5.84-11.30 μmol electrons m^{-2} s^{-1} (LC) to 10.69-12.45 μmol electrons m^{-2} s^{-1}. Furthermore, UVB significantly deteriorated the positive effects on Fv/Fm and α compared to PAR control treatment under both HC and LC. However, under LC treatment, I_k was significantly promoted from 153.39-237.07 μmol electrons m^{-2} s^{-1} (HC) to 235.52-783.04 μmol electrons m^{-2} s^{-1} and the lowest value of I_k was at HC+PAR.

3.4 Pigments and phycobiliprotein contents

OA had significant effects on the contents of Chl a and Car, but the interaction between OA and UVR had no significant effect (Supplementary Table S4). Compared to the PAR treatment, both Chl a and Car decreased under other UVR treatments regardless of LC and HC (Figures 4A, B). In addition, Chl a and Car contents were higher in HC than those in LC for all UVR treatments. Further, the highest contents of Chl a and Car were 5.76 and 1.41 mg g^{-1} at HC+PAR treatment, while the lowest contents were 0.72 and 0.20 mg g^{-1} at LC+PAR+UVB treatment. For PE and PC, only OA had a significant effect on their contents in *Rhodosorus* sp. SCSIO-45730 (Supplementary Table S4). Concerning LC treatments, the elevated pCO_2 induced the accumulation of PE and PC among all UVR treatments (Figures 4C, D). Under HC treatment, the contents of PE significantly increased from 15.40-17.76 mg g^{-1} (LC) to 28.83-36.88 mg g^{-1}, and PC from 4.82-6.15 mg g^{-1} (LC) to 7.84-8.30 mg g^{-1}.

3.5 Carbohydrate, protein and total lipids contents

The contents of carbohydrate, protein and total lipids were all significantly affected by OA under either PAR, PAR+UVA, or

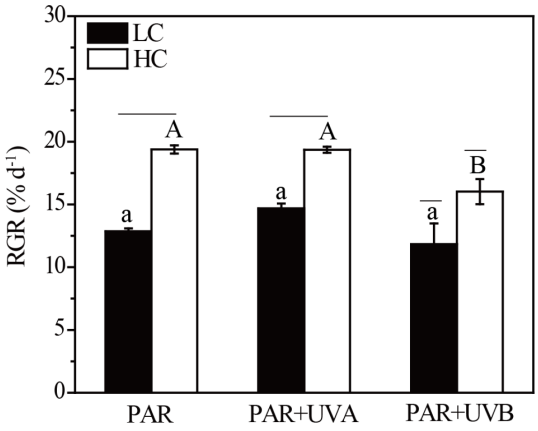

FIGURE 1
The relative growth rate (RGR) of *Rhodosorus* sp. SCSIO-45730 treated under different pCO_2 levels and UVR. Short horizontal lines represent significant differences (P<0.05) among CO_2 treatments at the same UVR treatment, while long horizontal lines indicate insignificant differences. Different lowercase letters represent significant differences (P<0.05) among UVR treatments under LC, and different capital letters indicate significant differences (P<0.05) among UVR treatments under HC.

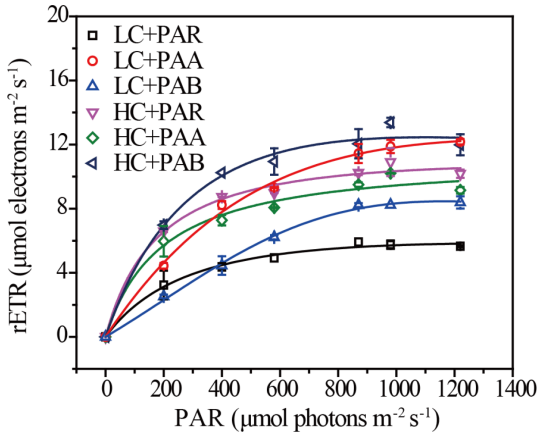

FIGURE 2
Rapid light curves (RLCs) of *Rhodosorus* sp. SCSIO-45730 under different pCO_2 levels and UVR.

PAR+UVB treatments (Supplementary Table S5). Under LC, the carbohydrate content of *Rhodosorus* sp. SCSIO-45730 significantly decreased by 23.05%, 20.35% and 36.05%, respectively at PAR, PAR+UVA and PAR+UVB conditions under HC (Figure 5A). The highest carbohydrate accumulation was found at HC+PAR (43.03% DW) among the six treatments. In contrast, under LC conditions, the contents of protein and total lipids increased from 20.72-25.54% DW (HC) to 29.34-34.24 % DW and from 8.86-13.16 % DW (HC) to 11.49-15.32 % DW, respectively (Figures 5B, C). In addition, UVR treatment was significant for the contents of carbohydrate, protein and total lipids (Supplementary Table S5). On the other hand, the contents of protein and total lipids were significantly promoted by UVB and their highest values of 34.25 and 15.32 % DW were observed at LC+PAR+UVB.

3.6 TC, TN contents and TC/TN ratios

Two-way ANOVA indicated that both OA and UVR had significant effects on total carbon, nitrogen contents and TC/TN ratios, and there was also a significant interaction between them (Supplementary Table S6). *Rhodosorus* sp. SCSIO-45730 accumulated TC under HC compared to LC treatments, with values of 36.99, 33.89 and 33.06 % DW at PAR, PAR+UVA or PAR+UVB conditions, respectively (Figure 6A). Moreover, PAR+UVA and PAR+UVB treatments significantly decreased TC content regardless of pCO_2 levels when compared with PAR conditions. Conversely, it is apparent that the elevated CO_2 significantly decreased the TN contents from 4.49-5.38 % DW (LC) to 2.32-3.52 % DW (Figure 6B). It is interesting to note that, compared to PAR treatments, PAR+UVA and PAR+UVB treatments significantly increased TN by 9.3% and 19.76%, respectively, under LC, while TN content also increased by 8.4% and 51.72%, respectively, under HC. As a result, the change in TC/TN ratios showed a similar trend to TC (Figure 6C). Under HC treatments, the TC/TN ratios ranged from 9.39 to 15.93, which was 63.87%-97.88% higher than the algae incubated under LC conditions (5.73-8.05). Additionally, PAR+UVA and PAR+UVB treatments conducted negative effects on TC/TN ratios.

3.7 Enzyme activities

The antioxidant enzyme activity, assessed using SOD and CAT, was shown in Figures 7A, B. The SOD activity of *Rhodosorus* sp. SCSIO-45730 was significantly influenced by UVR, while both OA and UVR and their interactions had significant effects on CAT activity (Supplementary Table S7). For SOD, the values under LC were significantly reduced by 38.01%, 46.02% and 54.94% on basis of HC under PAR, PAR+UVA and PAR+UVB treatments, respectively. In addition, the changing trend of OA and UVR on CAT activity of *Rhodosorus* sp. SCSIO-45730 was similar to that of SOD. On the whole, compared with the cell cultured under LC conditions, the CAT activity of algae under HC treatments was promoted from 0.35-2.23 IU mg^{-1} DW to 0.58-3.40 IU mg^{-1} DW. OA and UVR and their interactions also obviously affected the activities of CA and NR (Supplementary Table S7). The activities of CA and NR were higher in HC than in LC irrespective of UVR treatments (Figures 7C, D). Furthermore, the highest activities of CA and NR were pronounced in HC+PAR treatments, which showed values of 5.28 and 0.16 IU mg^{-1} DW, respectively.

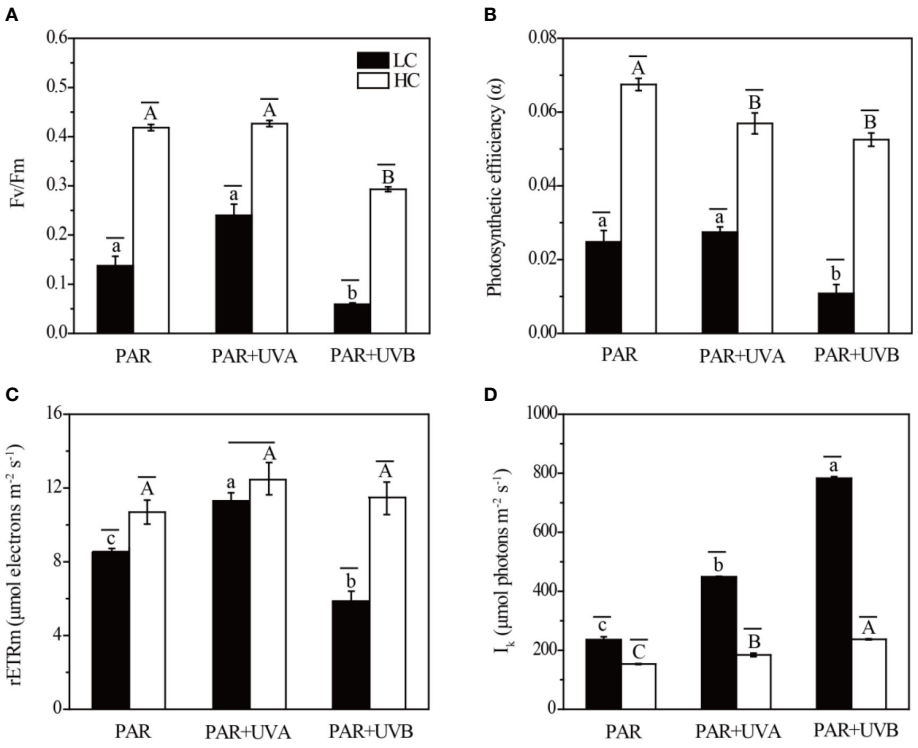

FIGURE 3
The photosynthetic parameters of *Rhodosorus* sp. SCSIO-45730 under different pCO_2 levels and UVR. **(A)** the optimal photochemical yield of PSII (Fv/Fm), **(B)** apparent photosynthetic efficiency (α), **(C)** maximum relative electron transport rate (rETRm), and **(D)** light saturation point (I_k). Short horizontal lines represent significant differences (P<0.05) among CO_2 treatments at the same UVR treatment, while long horizontal lines indicate insignificant differences. Different lowercase letters represent significant differences (P<0.05) among UVR treatments under LC, and different capital letters indicate significant differences (P<0.05) among UVR treatments under HC.

3.8 Phenols content

The phenols content under six treatments is presented in Figure 8. Supplementary Table S8 indicated that both OA and UVR significantly affected phenols content and they also had an interactive effect. Under HC treatments, the phenols contents of *Rhodosorus* sp. SCSIO-45730 were 2.09, 5.14 and 6.59 mg g^{-1} under PAR, PAR+UVA and PAR+UVB conditions, respectively, decreasing to 1.85, 1.90 and 3.20 mg g^{-1} under LC treatments, respectively.

4 Discussion

4.1 Effects of OA on growth, photosynthesis performances, biochemical compositions and enzyme activity of *Rhodosorus* sp. SCSIO-45730

OA has been reported to boost the growth and photosynthesis performances of some algae species, such as the genus *Ulva* (Xu et al., 2017), *Pyropia yezoensis* (Bao et al., 2019) and *Gracilariopsis lemaneiformis* (Wei et al., 2021), which was similar with our results. The elevated CO_2 levels significantly promoted the growth rate of *Rhodosorus* sp. SCSIO-45730 resulted from the alteration of the carbon concentrating mechanisms (CCMs). As we all know, most micro or macroalgae could use CCMs to meet the photosynthetic demand for inorganic carbon (Li et al., 2020a). Higher CO_2 concentration alleviated CO_2 limitation and decreased pH in the ocean, leading to reductions in algae CCM activities (Li et al., 2020c). Meanwhile, the down-regulation of CCMs could save up to 20% of energy and allow more remaining energy for biomass accumulation and photosynthesis rate enhancement (Zhou et al., 2022). Conversely, Li et al. (2020a) stated that the elevated CO_2 had obvious negative growth impacts on *Porphyra haitanensis*. Furthermore, there was no significant effect on the economic seaweed *Sargassum fusiforme* under normal cultivation (Jiang et al., 2019). Thus, these diverse differences in algae were probably caused by species-specific as well as the combination of OA and other environmental factors. Moreover, the present study found that elevated CO_2 positively increased the photosynthetic performances of *Rhodosorus* sp. SCSIO-45730, reflecting in higher Fv/Fm, α and rETRm coupling with

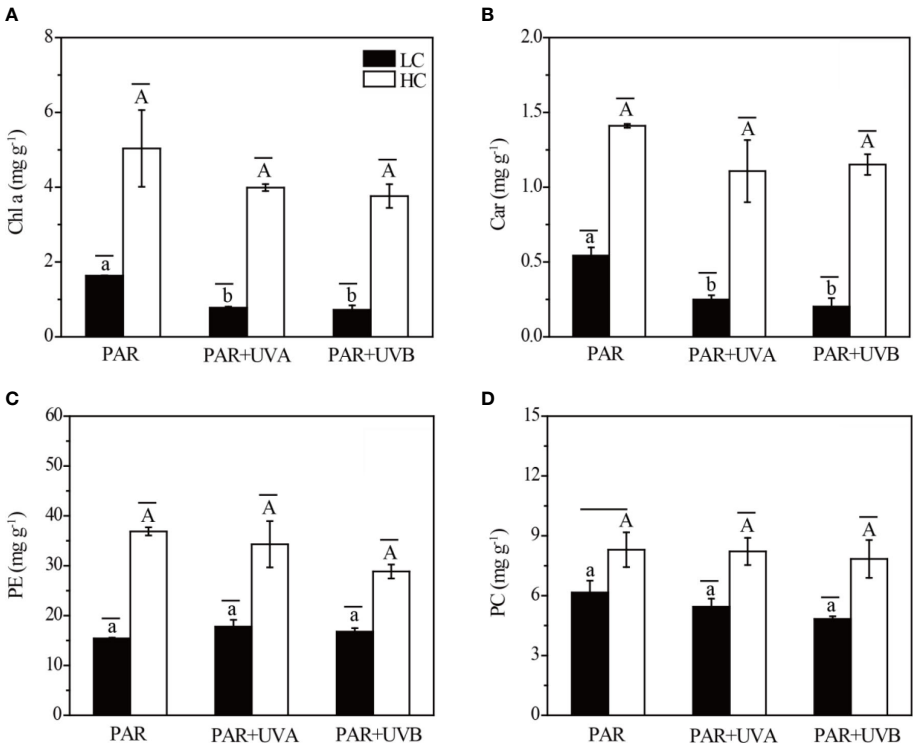

FIGURE 4
The Chl a **(A)**, Car **(B)**, PE **(C)** and PC **(D)** of *Rhodosorus* sp. SCSIO-45730 treated under different pCO_2 levels and UVR. Short horizontal lines represent significant differences (P<0.05) among CO_2 treatments at the same UVR treatment, while long horizontal lines indicate insignificant differences. Different lowercase letters represent significant differences (P<0.05) among UVR treatments under LC, and different capital letters indicate significant differences (P<0.05) among UVR treatments under HC.

increased contents of Chl a, Car, PE and PC, which could result from multiple acclimation mechanisms against OA. It is of note, that higher CO_2 concentration enhanced the carboxylation activity of RuBisCO but decreased its oxygenating activity, leading to better photosynthetic activity, and greater rETRm and α values in PSII were helpful for carbon fixation (Sheng et al., 2022). Fv/Fm represents the maximum potential of algae for photosynthesis and is also an important indicator to reflect the physiological status of algae. The higher Fv/Fm occurred as a response of *Rhodosorus* sp. SCSIO-45730 to OA, which conformed to the described in *Gracilariopsis lemaneiformis* under HC (Wei et al., 2021).

As earlier mentioned, enhanced photosynthetic performances and carbon fixation induced the formation of photosynthetic products, such as carbohydrate, protein and total lipids, *via* the Calvin cycle (Chen et al., 2018). Algae cells coped with environmental stress by regulating their physiological processes, so the increase of carbohydrate and decrease of protein and total lipids might be due to an acclimation response that sustained *Rhodosorus* sp. SCSIO-45730 to respond to OA, as some literature had previously reported. Wei et al. (2021) postulated that the CO_2 elevation caused soluble carbohydrate enhancement and protein decline in economically important red macroalga *Gracilariopsis lemaneiformis*. Similar phenomena were observed in several algae including *Pyropia haitanensis* (Chen et al., 2017), *Saccharina latissimi* (Olischläger et al., 2014) and *Ulva rigida* (Gordillo et al., 2001), resulting from down-regulated genes in photosynthetic pathway after carbohydrate accumulation. Moreover, previous evidence had shown that increasing CO_2 concentrations would induce changes in C and N accumulation processes, which resulted from CA and NR enzyme activities (Chen et al., 2017). In our study, *Rhodosorus* sp. SCSIO-45730 showed higher CA and NR activities compared to LC conditions, as well as higher TC and TC/TN ratios. It is possible that, on one hand, CA played a significant role in the transformation of CO_2 and HCO_3^-, on the other hand, NR activated NO_3^- uptake and N assimilation, and both of them favored C and N constituent enhancement at HC levels, which were in parallel with the literature reported by García-Sánchez et al. (1994) and

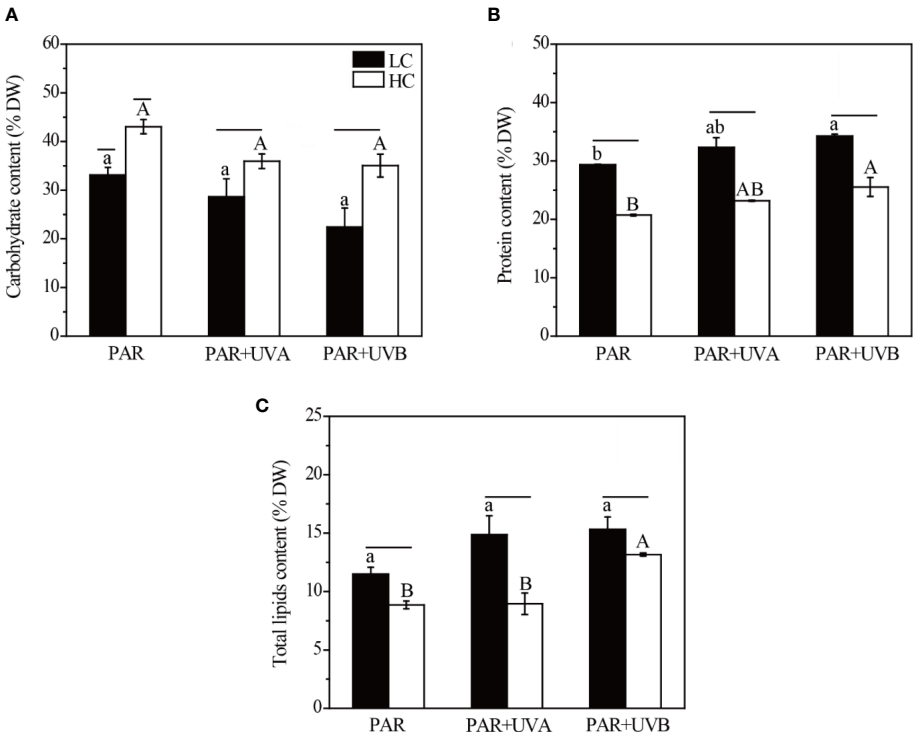

FIGURE 5
The carbohydrate **(A)**, protein **(B)** and total lipids **(C)** contents of *Rhodosorus* sp. SCSIO-45730 treated under different pCO_2 levels and UVR. Short horizontal lines represent significant differences (P<0.05) among CO_2 treatments at the same UVR treatment, while long horizontal lines indicate insignificant differences. Different lowercase letters represent significant differences (P<0.05) among UVR treatments under LC, and different capital letters indicate significant differences (P<0.05) among UVR treatments under HC.

Gordillo et al. (2001). Furthermore, the ratio of TC/TN was kept within certain balance limits under HC, leading to an increased synthesis of carbohydrate and pigments but a decrease in protein.

The rapid growth and increased photosynthesis of *Rhodosorus* sp. SCSIO-45730 led to greater ROS production, which potentially caused oxidative damage. SOD and CAT participate in the first line of defense against oxidative damage, which can reduce or scavenge the toxicity of free radicals and peroxides, and can improve the tolerance of algae to the environment under stress (Xia et al., 2018). The current study demonstrated that the elevated CO_2 promoted the increase of SOD and CAT activities, which was similar to the investigation of dinoflagellate *Karenia mikimotoi* under OA (Zhang et al., 2022). The marked increase in SOD activity in the algae might be attributed to the formation of H_2O_2, and the increased CAT effectively worked in the decomposition of H_2O_2 to H_2O and O_2 at the same time, protecting algae cells from OA stress (Wu et al., 2015). In addition, higher phenols and Car contents under HC also helped to quench ROS, eliminating peroxyl radicals and stabilizing intracellular oxidative homeostasis.

4.2 Effects of UVR on growth, photosynthesis performances, biochemical compositions and enzyme activity of *Rhodosorus* sp. SCSIO-45730

UVR is known to have negative effects on algae, such as destructing macromolecules, affecting the uptake of nutrients, inhibiting photosynthesis, reducing the growth rate, stimulating ROS formation and decreasing the primary production (Li et al., 2017). However, the present study showed that UVA had no significant effects on the growth of *Rhodosorus* sp. SCSIO-45730, on the other hand, UVB significantly inhibited its growth as compared to PAR treatments. Such a phenomenon was also described in *Phaeocystis globosa* (Chen and Gao, 2011) and *Gracilaria lemaneiformis* (Xu and Gao, 2010). UVA slightly promoted the RGR of *Rhodosorus* sp. SCSIO-45730 may be due to the limited PAR intensity used in this study, so the energy of UVA could be directly absorbed by Chl a and phycobiliproteins as light energy for algal photosynthetic carbon fixation (Bhandari and Sharma, 2006). The decreased growth rate caused by UVB can be the cost of cell damage repair (Otogo et al., 2021). The growth of

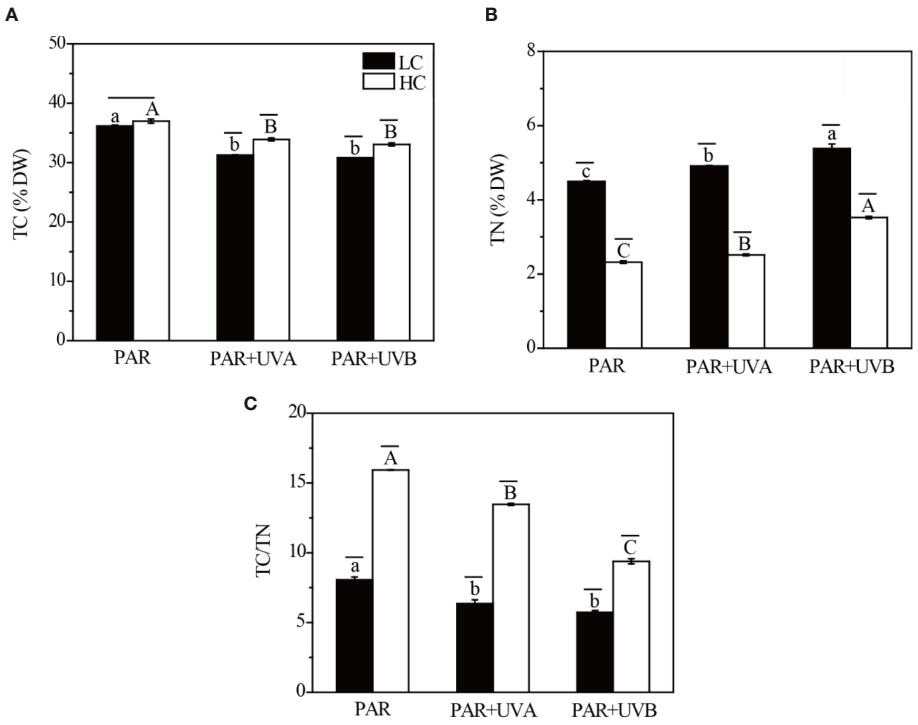

FIGURE 6
The TC **(A)**, TN **(B)** contents and TC/TN ratios **(C)** of *Rhodosorus* sp. SCSIO-45730 treated under different pCO_2 levels and UVR. Short horizontal lines represent significant differences (P<0.05) among CO_2 treatments at the same UVR treatment, while long horizontal lines indicate insignificant differences. Different lowercase letters represent significant differences (P<0.05) among UVR treatments under LC, and different capital letters indicate significant differences (P<0.05) among UVR treatments under HC.

Rhodosorus sp. SCSIO-45730 was closely related to photosynthesis parameters and photosynthetic pigments. Overall, UVA slightly promoted photosynthesis while UVB significantly inhibited photosynthesis. UVB caused a significant reduction of Fv/Fm and rETRm, while UVA resulted in much less positive stimulation regardless of LC and HC conditions. Also, *Rhodosorus* sp. SCSIO-45730 significantly increased the values of I_k after exposure to UVR. It can be estimated that significant photoinhibition was observed in algae upon UVB emergency, most likely associated with the destruction of PSII proteins. In addition, UVB blocks *de novo* synthesis of the D1 protein, affecting the function of cells to respond to functional impairment of PSII, thus inhibiting photosynthetic activities (Garcia-Gomez et al., 2016). Photosynthesis depends on the light-harvesting characteristics of chlorophyll, so pigment contents provide important elements related to the status of the photosynthetic apparatus (Kumar et al., 2018). As earlier mentioned, decreased contents of Chl a and Car were detected in *Karenia mikimotoi* under UVR (Halac et al., 2014), which corresponded to our results. Also, Figueroa et al. (2010) reported that UVR damaged and decreased the pigments of *Gracilaria conferta*. In brief, UVR negatively affects photosynthetic pigments by degrading or inhibiting enzymes involved in their biosynthetic pathways (Álvarez Gómez et al., 2019). There were no obvious differences in PE and PC contents among PAR, PAR+UVA and PAR+UVB, which may be attributed to the algae resilience to UVR exposure.

Marine algae can repair UV-induced damage by a variety of mechanisms, many of which involve changes in the content of bioactive compounds, such as carbohydrate, protein, and total lipids. Carbohydrate contents decreased slightly under UVA and UVB treatments, that was because UVR caused damage to thylakoids of the chloroplast, and the generation of free radicals led to a content decrease (Álvarez Gómez et al., 2019). With respect to protein content, UVB significantly promoted its accumulation, which was in accordance with the results in *Porphyra haitanensis* (Otogo et al., 2021), *Scenedesmus acutus* (Fu et al., 2021) and *Microcystis flos-aquae* (El-Sheekh et al., 2021), resulting from protein damage and the cellular demands required to maintain homeostasis and photosynthetic processes. On the other hand, UV radiation-induced protein accumulation protected algae from UVR-promoted peroxidative processes. In addition, UVR also positively induced the production of total

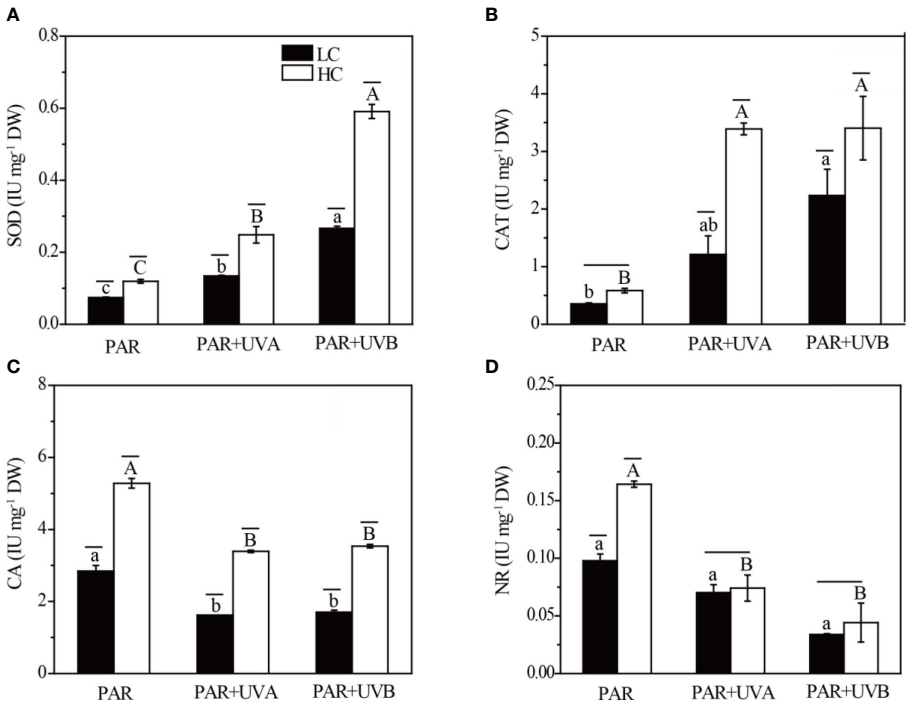

FIGURE 7
The activities of SOD **(A)**, CAT **(B)**, CA **(C)** and NR **(D)** of *Rhodosorus* sp. SCSIO-45730 treated under different pCO_2 levels and UVR. Short horizontal lines represent significant differences (P<0.05) among CO_2 treatments at the same UVR treatment, while long horizontal lines indicate insignificant differences. Different lowercase letters represent significant differences (P<0.05) among UVR treatments under LC, and different capital letters indicate significant differences (P<0.05) among UVR treatments under HC.

lipids. Casazza et al. (2015) reported that UV treatment led to increasing the lipid content by 29.5% for *Arthrospira (Spirulina) platensis* compared to the control run, which agreed with the opinion that microalgae can accumulate lipids under stress conditions. It had been widely accepted that alterations in TC and TN contents of algae under UV conditions were indicative of the coupling between C and N absorption and assimilation processes, as well as C:N balance (Narvarte et al., 2020). Meanwhile, UVR could negatively affect the activities of CA and NR, suppressing the carbon and nutrients uptaking (Li et al., 2017). In our test, changes in TC and TN corresponded to alterations in carbohydrate, protein and total lipids contents, leading to a decrease in TC/TN under UVR treatments.

Literature reported that UVR induced the accumulation of ROS, and marine algae developed strategies to block UVR damage and preserve cellular integrity (Rastogi et al., 2020). Additionally, UVR increased the activities of SOD and CAT, thereby regulating homeostatic balance in algal cells against UV-induced oxidative damage. UVR also induced the production of antioxidants, such as phenolic compounds, which helped to counteract the detrimental effects of UVR, and such phenomena were also observed in *Ulva rigida* (Cabello-Pasini et al., 2011) and *Acanthophora spicifera* (Pereira et al., 2019).

4.3 The interactive effects of OA and UVR

Recent research showed the effects of OA on phytoplankton were modulated by many global change factors, especially UVR (Li et al., 2022a). Revealing the complicated interactions between OA and UVR is crucial for predicting the effects of climate change on marine algae. Additionally, the combined effects of OA and UVR were different from species to species. For instance, it has been established that elevated CO_2 may act synergistically to enhance the harmful effects on *Emiliania huxleyi* under UVR or both together to stimulate the growth of primary producers (Gao et al., 2009). Moreover, the elevated CO_2 partly counteracted UVR-induced damage on *Phaeodactylum tricornutum* (Li et al., 2012), *Chaetoceros curvisetus* (Chen et al., 2015) and *Dunaliella tertiolecta* (Garcia-Gomez et al., 2014). Our study about the combined effects of OA and UVR on biochemical compositions and photosynthetic performances of *Rhodosorus* sp. SCSIO-45730 stated the deleterious effects of UVR on algae were significantly ameliorated by OA, especially in terms of Fv/Fm, rETRm, I_k, TC, TN, TC/TN, phenols contents, and the activities of CAT, CA and NR. OA helped to relieve the UVR-related photochemical inhibition and repair UV-induced damage, that is to say, the

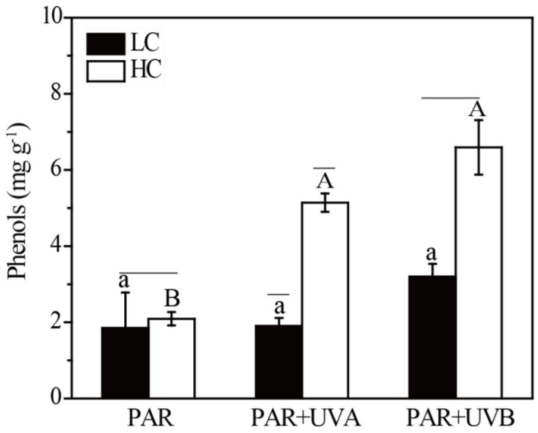

FIGURE 8
The phenols content of *Rhodosorus* sp. SCSIO-45730 treated under different pCO_2 levels and UVR. Short horizontal lines represent significant differences (P<0.05) among CO_2 treatments at the same UVR treatment, while long horizontal lines indicate insignificant differences. Different lowercase letters represent significant differences (P<0.05) among UVR treatments under LC, and different capital letters indicate significant differences (P<0.05) among UVR treatments under HC.

elevated CO_2 endowed algae with higher resistance to UVR. Such results might result from the species-specific CCM efficiency of different phytoplankton, which could affect the energy balance of algae cells. In detail, OA reduced CCM activity and released additional energy to help promote the repair of UVR damage, especially UVB, which was in line with the response of *Ulva linza* exposure to both OA and UVR (Ma et al., 2019).

5 Conclusion

This study details that UVR and OA could individually or interactively impact the growth, photosynthesis parameters, biochemical compositions and enzyme activity of *Rhodosorus* sp. SCSIO-45730. It showed that the UVA had no significant effects on the growth of this strain, while UVB exposure had a significant negative effect. Additionally, OA could alleviate the detrimental effects on growth rates, especially for UVB by boosting its photosynthetic pigments contents and photosynthetic efficiency, suggesting the primary productivity of this marine algae will benefit from OA in the future. Moreover, carbohydrate contents, total carbon, TC/TN ratio, as well as phenols content of *Rhodosorus* sp. SCSIO-45730 elevated related to the increase of CAA, NAR, SOD and CAT under HC. However, UVR damaged various important macromolecules, making algal cells need more energy to repair themselves. Simultaneously, the above responses of *Rhodosorus* sp. SCSIO-45730 resulted from OA and ultimately promoted its resilience to UVB *via* repairing UVR damage. This finding suggested that *Rhodosorus* sp. would benefit from the future scenarios of global change and become a winner species. To better simulate the actual ocean environment in the future, we would perform an outdoor semi-continuous culture, which may provide a better understanding of the algal response to the dynamic changing climate (Bao et al., 2019). In addition, except for the enhancement of OA and UVR, multiple other environmental factors are driven by the progressive ocean global changes, such as nutrient level, temperature, heatwaves, salinity and deoxygenation. Therefore, it is necessary to further understand the multi-factor effects of OA and other climate change-relevant factors on *Rhodosorus* sp. SCSIO-45730, and provide guidance for its commercial culture in coastal areas.

Data availability statement

The raw data supporting the conclusions of this article will be made available by the authors, without undue reservation.

Author contributions

NW: Methodology, software, writing-original draft. JL: Investigation, methodology. FY, TL and HuW: Writing – review & editing. CL, HP and HoW: Resources. WX: Conceptualization, project administration, resources. All authors contributed to the article and approved the submitted version.

Funding

This research was supported by Key-Area Research and Development Program of Guangdong Province (2020B1111030004), Key Special Project for Introduced Talents Team of Southern Marine Science and Engineering Guangdong Laboratory (Guangzhou)

(GML2019ZD0406), and Science and Technology Planning Project of Guangdong Province of China (2019B030316027).

Acknowledgments

The authors thank all of the members for their support for the study.

Conflict of interest

The authors declare that the research was conducted in the absence of any commercial or financial relationships that could be construed as a potential conflict of interest.

Publisher's note

All claims expressed in this article are solely those of the authors and do not necessarily represent those of their affiliated organizations, or those of the publisher, the editors and the reviewers. Any product that may be evaluated in this article, or claim that may be made by its manufacturer, is not guaranteed or endorsed by the publisher.

Supplementary material

The Supplementary Material for this article can be found online at: https://www.frontiersin.org/articles/10.3389/fmars.2022.1092451/full#supplementary-material

References

Álvarez Gómez, F., Korbee, N., and Figueroa, F. L. (2019). Effects of UV radiation on photosynthesis, antioxidant capacity and the accumulation of bioactive compounds in *Gracilariopsis longissima*, *Hydropuntia cornea* and *Halopithys incurva* (Rhodophyta). *J. Phycol.* 55 (6), 1258–1273. doi: 10.1111/jpy.12899

Bao, M., Wang, J., Xu, T., Wu, H., Li, X., and Xu, J. (2019). Rising CO_2 levels alter the responses of the red macroalga *Pyropia yezoensis* under light stress. *Aquac* 501, 325–330. doi: 10.1016/j.aquaculture.2018.11.011

Bhandari, R., and Sharma, P. K. (2006). High-light-induced changes on photosynthesis, pigments, sugars, lipids and antioxidant enzymes in freshwater (*Nostoc spongiaeforme*) and marine (*Phormidium corium*) cyanobacteria. *Photochem. Photobiol.* 82 (3), 702–710. doi: 10.1562/2005-09-20-RA-690

Cabello-Pasini, A., Macías-Carranza, V., Abdala, R., Korbee, N., and Figueroa, F. L. (2011). Effect of nitrate concentration and UVR on photosynthesis, respiration, nitrate reductase activity, and phenolic compounds in *Ulva rigida* (Chlorophyta). *J. Appl. Psychol.* 23 (3), 363–369. doi: 10.1007/s10811-010-9548-0

Casazza, A. A., Ferrari, P. F., Aliakbarian, B., Converti, A., and Perego, P. (2015). Effect of UV radiation or titanium dioxide on polyphenol and lipid contents of arthrospira (Spirulina) platensis. *Algal Res.* 12, 308–315. doi: 10.1016/j.algal.2015.09.012

Chen, S., and Gao, K. (2011). Solar ultraviolet radiation and CO_2-induced ocean acidification interacts to influence the photosynthetic performance of the red tide alga *Phaeocystis globosa* (Prymnesiophyceae). *Hydrobiologia* 675 (1), 105–117. doi: 10.1007/s10750-011-0807-0

Chen, H., Guan, W., Zeng, G., Li, P., and Chen, S. (2015). Alleviation of solar ultraviolet radiation (UVR)-induced photoinhibition in diatom *Chaetoceros curvisetus* by ocean acidification. *J. Mar. Biol. Assoc. UK.* 95 (4), 661–667. doi: 10.1017/S0025315414001568

Chen, B., Zou, D., Du, H., and Ji, Z. (2018). Carbon and nitrogen accumulation in the economic seaweed *Gracilaria lemaneiformis* affected by ocean acidification and increasing temperature. *Aquac* 482, 176–182. doi: 10.1016/j.aquaculture.2017.09.042

Chen, B., Zou, D., and Yang, Y. (2017). Increased iron availability resulting from increased CO_2 enhances carbon and nitrogen metabolism in the economical marine red macroalga *Pyropia haitanensis* (Rhodophyta). *Chemosphere* 173, 444–451. doi: 10.1016/j.chemosphere.2017.01.073

Dai, L., Tan, L., Jin, X., Wu, H., Wu, H., Li, T., et al. (2020). Evaluating the potential of carbohydrate-rich microalga rhodosorus sp. SCSIO-45730 as a feedstock for biofuel and β-glucans using strategies of phosphate optimization and low-cost harvest. *J. Appl. Psychol.* 32 (5), 3051–3061. doi: 10.1007/s10811-020-02139-8

Davison, I. R., Jordan, T. L., Fegley, J. C., and Grobe, C. W. (2007). Response of *Laminaria saccharina* (Phaeophyta) growth and photosynthesis to simultaneous ultraviolet radiation and nitrogen limitation. *J. Phhycol.* 43 (4), 636–646. doi: 10.1111/j.1529-8817.2007.00360.x

Dubois, M., Gilles, K. A., Hamilton, J. K., Rebers, P. T., and Smith, F. (1956). Colorimetric method for determination of sugars and related substances. *Anal. Chem.* 28 (3), 350–356. doi: 10.1021/ac60111a017

Eilers, P. H. C., and Peeters, J. C. H. (1988). A model for the relationship between light intensity and the rate of photosynthesis in phytoplankton. *Ecol. Model.* 42 (3-4), 199–215. doi: 10.1016/0304-3800(88)90057-9

El-Sheekh, M. M., Alwaleed, E. A., Ibrahim, A., and Saber, H. (2021). Detrimental effect of UV-b radiation on growth, photosynthetic pigments, metabolites and ultrastructure of some cyanobacteria and freshwater chlorophyta. *Int. J. Radiat. Biol.* 97 (2), 265–275. doi: 10.1080/09553002.2021.1851060

Figueroa, F. L., Israel, A., Neori, A., Martínez, B., Malta, E. J., Put, A., et al. (2010). Effect of nutrient supply on photosynthesis and pigmentation to short-term stress (UV radiation) in *Gracilaria conferta* (Rhodophyta). *Mar. pollut. Bull.* 60 (10), 1768–1778. doi: 10.1016/j.marpolbul.2010.06.009

Foo, S. C., Yusoff, F. M., Ismail, M., Basri, M., Yau, S. K., Khong, N. M., et al. (2017). Antioxidant capacities of fucoxanthin-producing algae as influenced by their carotenoid and phenolic contents. *J. Biotechnol.* 241, 175–183. doi: 10.1016/j.jbiotec.2016.11.026

Fu, S., Xue, S., Chen, J., Shang, S., Xiao, H., Zang, Y., et al. (2021). Effects of different short-term UV-b radiation intensities on metabolic characteristics of *Porphyra haitanensis*. *Int. J. Mol. Sci.* 22 (4), 2180. doi: 10.3390/ijms22042180

Gao, G., Beardall, J., Bao, M., Wang, C., Ren, W., and Xu, J. (2018). Ocean acidification and nutrient limitation synergistically reduce growth and photosynthetic performances of a green tide alga *Ulva linza*. *Biogeosciences* 15 (11), 3409–3420. doi: 10.5194/bg-15-3409-2018

Gao, K., Gao, G., Wang, Y., and Dupont, S. (2020). Impacts of ocean acidification under multiple stressors on typical organisms and ecological processes. *Mar. Life Sci. Tech.* 2 (3), 279–291. doi: 10.1007/s42995-020-00048-w

Gao, K., Ruan, Z., Villafane, V. E., Gattuso, J. P., and Helbling, E. W. (2009). Ocean acidification exacerbates the effect of UV radiation on the calcifying phytoplankter *Emiliania huxleyi*. *Limnol. Oceanogr.* 54 (6), 1855–1862. doi: 10.4319/lo.2009.54.6.1855

Gao, K., and Zheng, Y. (2010). Combined effects of ocean acidification and solar UV radiation on photosynthesis, growth, pigmentation and calcification of the coralline alga *Corallina sessilis* (Rhodophyta). *Global Change Biol.* 16 (8), 2388–2398. doi: 10.1111/j.1365-2486.2009.02113.x

Garcia-Gomez, C., Gordillo, F. J., Palma, A., Lorenzo, M. R., and Segovia, M. (2014). Elevated CO_2 alleviates high PAR and UV stress in the unicellular chlorophyte *Dunaliella tertiolecta*. *Photoch. Photobio. Sci.* 13 (9), 1347–1358. doi: 10.1039/c4pp00044g

Garcia-Gomez, C., Mata, M. T., Van Breusegem, F., and Segovia, M. (2016). Low-steady-state metabolism induced by elevated CO_2 increases resilience to UV radiation in the unicellular green-algae *Dunaliella tertiolecta*. *Environ. Exp. Bot.* 132, 163–174. doi: 10.1016/j.envexpbot.2016.09.001

García-Sánchez, M. J., Fernández, J. A., and Niell, X. (1994). Effect of inorganic carbon supply on the photosynthetic physiology of *Gracilaria tenuistipitata*. *Planta* 194 (1), 55–61. doi: 10.1007/BF00201034

Gordillo, F. J., Niell, F. X., and Figueroa, F. L. (2001). Non-photosynthetic enhancement of growth by high CO_2 level in the nitrophilic seaweed *Ulva rigida* c. agardh (Chlorophyta). *Planta* 213 (1), 64–70. doi: 10.1007/s004250000468

Guan, W., Si, R., Li, X., Cai, J., and Chen, S. (2018). Interactive effect of nitrogen source and high CO_2 concentration on the growth of the dinoflagellate *Alexandrium tamarense* and its toxicity to zebrafish (*Danio rerio*) embryos. *Mar. pollut. Bull.* 133, 626–635. doi: 10.1016/j.marpolbul.2018.06.024

Halac, S. R., Villafañe, V. E., Gonçalves, R. J., and Helbling, E. W. (2014). Photochemical responses of three marine phytoplankton species exposed to ultraviolet radiation and increased temperature: role of photoprotective mechanisms. *J. Photoch. Photobio. B.* 141, 217–227. doi: 10.1016/j.jphotobiol.2014.09.022

Jiang, X., Zhang, Y., Hutchins, D. A., and Gao, K. (2022). Nitrogen-limitation exacerbates the impact of ultraviolet radiation on the coccolithophore *Gephyrocapsa oceanica*. *J. Photoch. Photobio. B.* 226, 112368. doi: 10.1016/j.jphotobiol.2021.112368

Jiang, H., Zou, D., Lou, W., and Gong, J. (2019). Effects of CO_2 supply on growth and photosynthetic ability of young sporophytes of the economic seaweed *Sargassum fusiforme* (Sargassaceae, phaeophyta). *J. Phhycol.* 31 (1), 615–624. doi: 10.1007/s10811-018-1569-0

Ji, Y., and Gao, K. (2021). Effects of climate change factors on marine macroalgae: a review. *Adv. Mar. Biol.* 88, 91–136. doi: 10.1016/bs.amb.2020.11.001

Khozin-Goldberg, I., Shrestha, P., and Cohen, Z. (2005). Mobilization of arachidonyl moieties from triacylglycerols into chloroplastic lipids following recovery from nitrogen starvation of the microalga *Parietochloris incisa*. *BBA-Mol. Cell Biol. L.* 1738 (1-3), 63–71. doi: 10.1016/j.bbalip.2005.09.005

Kumar, V., Nanda, M., Kumar, S., and Chauhan, P. K. (2018). The effects of ultraviolet radiation on growth, biomass, lipid accumulation and biodiesel properties of microalgae. *Energy Sources Part A.* 40 (7), 787–793. doi: 10.1080/15567036.2018.1463310

Liang, C., Zhang, Y., Wang, L., Shi, L., Xu, D., Zhang, X., et al. (2020). Features of metabolic regulation revealed by transcriptomic adaptions driven by long-term elevated p CO_2 in *Chaetoceros muelleri*. *Phycol. Res.* 68 (3), 236–248. doi: 10.1111/pre.12423

Li, T., Chen, Z., Wu, J., Wu, H., Yang, B., Dai, L., et al. (2020b). The potential productivity of the microalga, *Nannochloropsis oceanica* SCS-1981, in a solar powered outdoor open pond as an aquaculture feed. *Algal Res.* 46, 101793. doi: 10.1016/j.algal.2020.101793

Li, W., Gao, K., and Beardall, J. (2012). Interactive effects of ocean acidification and nitrogen-limitation on the diatom *Phaeodactylum tricornutum*. *PloS One* 7 (12), e51590. doi: 10.1371/annotation/98908e14-e9fd-458f-9cea-ba4bec139f20

Li, F., Li, H., Xu, T., Li, S., and Xu, J. (2022a). Seawater acidification exacerbates the negative effects of UVR on growth of the bloom-forming diatom *Skeletonema costatum*. *Front. Mar. Sci.* 878. doi: 10.3389/fmars.2022.905255

Li, G., Mai, G., Zhang, J., Lin, Q., Ni, G., Tan, Y., et al. (2020a). Algal density alleviates the elevated CO_2-caused reduction on growth of *Porphyra haitanensis* (Bangiales, rhodophyta), a species farmed in China. *Aquac. Res.* 51 (9). doi: 10.3389/fmars.2022.905255

Liu, C., Zou, D., Liu, Z., and Ye, C. (2020). Ocean warming alters the responses to eutrophication in a commercially farmed seaweed, *Gracilariopsis lemaneiformis*. *Hydrobiologia* 847 (3), 879–893. doi: 10.1007/s10750-019-04148-2

Li, W., Wang, T., Campbell, D. A., and Gao, K. (2020c). Ocean acidification interacts with variable light to decrease growth but increase particulate organic nitrogen production in a diatom. *Mar. Environ. Res.* 160, 104965. doi: 10.1016/j.marenvres.2020.104965

Li, W., Yang, Y., Li, Z., Xu, J., and Gao, K. (2017). Effects of seawater acidification on the growth rates of the diatom *Thalassiosira (Conticribra) weissflogii* under different nutrient, light, and UV radiation regimes. *J. Phycol.* 29 (1), 133–142. doi: 10.1007/s10811-016-0944-y

Li, H. Y., Yi, Y. L., Guo, S., Zhang, F., Yan, H., Zhan, Z. L., et al. (2022b). Isolation, structural characterization and bioactivities of polysaccharides from *Laminaria japonica*: A review. *Food Chem.* 370, 131010. doi: 10.1016/j.foodchem.2021.131010

Lowry, O. H. (1951). Protein measurement with the folin phenol reagent. *J. Biol. Chem.* 193, 265–275.

Ma, J., Wang, W., Qu, L., Liu, X., Wang, Z., Qiao, S., et al. (2019). Differential photosynthetic response of a green tide alga *Ulva linza* to ultraviolet radiation, under short- and long- term ocean acidification regimes. *Photochem. Photobiol.* 95 (4), 990–998. doi: 10.1111/php.13083

Narvarte, B. C. V., Nelson, W. A., and Roleda, M. Y. (2020). Inorganic carbon utilization of tropical calcifying macroalgae and the impacts of intensive mariculture-derived coastal acidification on the physiological performance of the rhodolith sporolithon sp. *Environ. pollut.* 266, 115344. doi: 10.1016/j.envpol.2020.115344

Olischläger, M., Iniguez, C., Gordillo, F. J. L., and Wiencke, C. (2014). Biochemical composition of temperate and Arctic populations of *Saccharina latissima* after exposure to increased pCO_2 and temperature reveals ecotypic variation. *Planta* 240 (6), 1213–1224. doi: 10.1007/s00425-014-2143-x

Otogo, R. A., Chia, M. A., Uyovbisere, E. E., Iortsuun, D. N., and do Carmo Bittencourt-Oliveira, M. (2021). Effect of ultraviolet radiation (type b) and titanium dioxide nanoparticles on the interspecific interaction between *Microcystis flos-aquae* and *Pseudokirchneriella subcapitata*. *Sci. Total Environ.* 779, 146561. doi: 10.1016/j.scitotenv.2021.146561

Pereira, D. T., Pereira, B., Fonseca, A., Ramlov, F., Maraschin, M., Álvarez-Gómez, F., et al. (2019). Effects of ultraviolet radiation (UV-a+ UV-b) on the antioxidant metabolism of the red macroalga species *Acanthophora spicifera* (Rhodophyta, ceramiales) from different salinity and nutrient conditions. *Photochem. Photobiol.* 95 (4), 999–1009. doi: 10.1111/php.13094

Pierrot, D., Lewis, E., and Wallace, D. W. R. (2006). *MS excel program developed for CO2 system calculations. ORNL/CDIAC-105a* (Oak Ridge, Tennessee: Carbon dioxide information analysis center, oak ridge national laboratory, US Department of Energy), 10.

Raposo, M. F., De Morais, R. M. S. C., and de Morais, A. M. M. B. (2013). Bioactivity and applications of sulphated polysaccharides from marine microalgae. *Mar. Drugs* 11 (1), 233–252. doi: 10.3390/md11010233

Rastogi, R. P., Madamwar, D., Nakamoto, H., and Incharoensakdi, A. (2020). Resilience and self-regulation processes of microalgae under UV radiation stress. *J. Photoch. Photobio. C.* 43, 100322. doi: 10.1016/j.jphotochemrev.2019.100322

Sero, E. T., Siziba, N., Bunhu, T., Shoko, R., and Jonathan, E. (2020). Biophotonics for improving algal photobioreactor performance: a review. *Int. J. Energ. Res.* 44 (7), 5071–5092. doi: 10.1002/er.5059

Sheng, Y., Mathimani, T., Brindhadevi, K., Basha, S., Elfasakhany, A., Xia, C., et al. (2022). Combined effect of CO_2 concentration and low-cost urea repletion/starvation in *Chlorella vulgaris* for ameliorating growth metrics, total and non-polar lipid accumulation and fatty acid composition. *Sci. Total Environ.* 808, 151969. doi: 10.1016/j.scitotenv.2021.151969

Sun, Z., Chen, Y. F., and Du, J. (2016). Elevated CO_2 improves lipid accumulation by increasing carbon metabolism in *Chlorella sorokiniana*. *Plant Biotechnol. J.* 14 (2), 557–566. doi: 10.1111/pbi.12398

Tandeau de Marsac, N., and Houmard, J. (1988). Complementary chromaticadaptation: Physiological conditions and action spectra. *Method Enzymol.*167, 318–328.

Wang, N., Chen, Z., Lv, J., Li, T., Wu, H., Wu, J., et al. (2022a). Characterization, hypoglycemia and antioxidant activities of polysaccharides from rhodosorus sp. SCSIO-45730. *Ind. Crop Prod.* 191 (2023), 115936. doi: 10.1016/j.indcrop.2022.115936

Wang, N., Dai, L., Chen, Z., Li, T., Wu, J., Wu, H., et al. (2022b). Extraction optimization, physicochemical characterization, and antioxidant activity of polysaccharides from rhodosorus sp. SCSIO-45730. *J. Appl. Psychol.* 34 (1), 285–299. doi: 10.1007/s10811-021-02646-2

Wei, Z., Zhang, Y., Yang, F., Liang, J., and Long, L. (2021). Increased light availability modulates carbon and nitrogen accumulation in the macroalga *Gracilariopsis lemaneiformis* (Rhodophyta) in response to ocean acidification. *Environ. Exp. Bot.* 187, 104492. doi: 10.1016/j.envexpbot.2021.104492

Wu, X., Gao, G., Giordano, M., and Gao, K. (2012). Growth and photosynthesis of a diatom grown under elevated CO_2 in the presence of solar UV radiation. *Fundam. Appl. Limnol.* 180 (4), 279. doi: 10.1127/1863-9135/2012/0299

Wu, H., Jiang, H., Liu, C., and Deng, Y. (2015). Growth, pigment composition, chlorophyll fluorescence and antioxidant defenses in the red alga *Gracilaria lemaneiformis* (Gracilariales, rhodophyta) under light stress. *S. Afr. J. Bot.* 100, 27–32. doi: 10.1016/j.sajb.2015.05.017

Xia, B., Sui, Q., Sun, X., Han, Q., Chen, B., Zhu, L., et al. (2018). Ocean acidification increases the toxic effects of TiO_2 nanoparticles on the marine microalga *Chlorella vulgaris*. *J. Hazard. Mater.* 346, 1–9. doi: 10.1016/j.jhazmat.2017.12.017

Xu, J., and Gao, K. (2010). UV-A enhanced growth and UV-b induced positive effects in the recovery of photochemical yield in *Gracilaria lemaneiformis* (Rhodophyta). *J. Photochem. Photobiol. B.* 100 (3), 117–122. doi: 10.1016/j.jphotobiol.2010.05.010

Xu, D., Schaum, C. E., Lin, F., Sun, K., Munroe, J. R., Zhang, X. W., et al. (2017). Acclimation of bloom-forming and perennial seaweeds to elevated pCO_2 conserved across levels of environmental complexity. *Global Change Biol.* 23 (11), 4828–4839. doi: 10.1111/gcb.13701

Yu, J., Tian, J. Y., Gao, G., Xu, R., Lai, J. G., and Yang, G. P. (2022). Growth, DMS and DMSP production in *Emiliania huxleyi* under elevated CO_2 and UV radiation. *Environ. pollut.* 294, 118643. doi: 10.1016/j.envpol.2021.118643

Zhang, J., Liu, L., Ren, Y., and Chen, F. (2019). Characterization of exopolysaccharides produced by microalgae with antitumor activity on human colon cancer cells. *Int. J. Biol. Macromol.* 128, 761–767. doi: 10.1016/j.ijbiomac.2019.02.009

Zhang, J., Yang, Q., Liu, Q., Liu, S., Zhu, Y., Yao, J., et al. (2022). The responses of harmful dinoflagellate *Karenia mikimotoi* to simulated ocean acidification at the transcriptional level. *Harm. Algae* 111, 102167. doi: 10.1016/j.hal.2021.102167

Zhou, W., Wu, H., Huang, J., Wang, J., Zhen, W., Wang, J., et al. (2022). Elevated-CO_2 and nutrient limitation synergistically reduce the growth and photosynthetic performances of a commercial macroalga *Gracilariopsis lemaneiformis*. *Aquaculture* 550, 737878. doi: 10.1016/j.aquaculture.2021.737878